

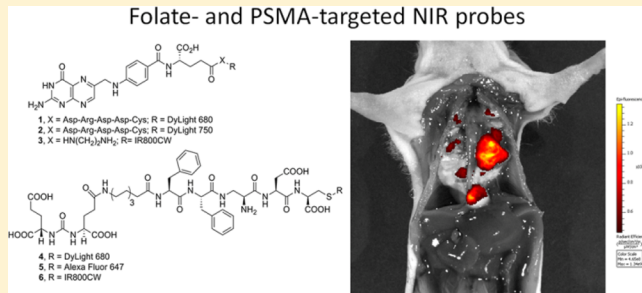
Development of Tumor-Targeted Near Infrared Probes for Fluorescence Guided Surgery

Lindsay E. Kelderhouse,[†] Venkatesh Chelvam,^{†,‡} Charity Wayua,[†] Sakkarapalayam Mahalingam,[†] Scott Poh,[†] Sumith A. Kularatne,^{†,§} and Philip S. Low*,[†]

[†]Department of Chemistry, Purdue University, 560 Oval Drive, West Lafayette, Indiana 47907, United States

Supporting Information

ABSTRACT: Complete surgical resection of malignant disease is the only reliable method to cure cancer. Unfortunately, quantitative tumor resection is often limited by a surgeon's ability to locate all malignant disease and distinguish it from healthy tissue. Fluorescence-guided surgery has emerged as a tool to aid surgeons in the identification and removal of malignant lesions. While nontargeted fluorescent dyes have been shown to passively accumulate in some tumors, the resulting tumor-to-background ratios are often poor, and the boundaries between malignant and healthy tissues can be difficult to define. To circumvent these problems, our laboratory has developed high affinity tumor targeting ligands that bind to receptors that are overexpressed on cancer cells and deliver attached molecules selectively into these cells. In this study, we explore the use of two tumor-specific targeting ligands (i.e., folic acid that targets the folate receptor (FR) and DUPA that targets prostate specific membrane antigen (PSMA)) to deliver near-infrared (NIR) fluorescent dyes specifically to FR and PSMA expressing cancers, thereby rendering only the malignant cells highly fluorescent. We report here that all FR- and PSMA-targeted NIR probes examined bind cultured cancer cells in the low nanomolar range. Moreover, upon intravenous injection into tumor-bearing mice with metastatic disease, these same ligand–NIR dye conjugates render receptor-expressing tumor tissues fluorescent, enabling their facile resection with minimal contamination from healthy tissues.



Complete surgical resection of malignant disease is the only reliable method to cure cancer. Unfortunately, quantitative tumor resection is often limited by a surgeon's ability to locate all malignant disease and distinguish it from healthy tissue. Fluorescence-guided surgery has emerged as a tool to aid surgeons in the identification and removal of malignant lesions. While nontargeted fluorescent dyes have been shown to passively accumulate in some tumors, the resulting tumor-to-background ratios are often poor, and the boundaries between malignant and healthy tissues can be difficult to define. To circumvent these problems, our laboratory has developed high affinity tumor targeting ligands that bind to receptors that are overexpressed on cancer cells and deliver attached molecules selectively into these cells. In this study, we explore the use of two tumor-specific targeting ligands (i.e., folic acid that targets the folate receptor (FR) and DUPA that targets prostate specific membrane antigen (PSMA)) to deliver near-infrared (NIR) fluorescent dyes specifically to FR and PSMA expressing cancers, thereby rendering only the malignant cells highly fluorescent. We report here that all FR- and PSMA-targeted NIR probes examined bind cultured cancer cells in the low nanomolar range. Moreover, upon intravenous injection into tumor-bearing mice with metastatic disease, these same ligand–NIR dye conjugates render receptor-expressing tumor tissues fluorescent, enabling their facile resection with minimal contamination from healthy tissues.

INTRODUCTION

Surgical removal of malignant disease constitutes one of the most common and effective treatments for cancer. Resection of all detectable malignant lesions cures approximately 50% of all cancer patients¹ and may extend life expectancy or reduce morbidity for others who eventually recur.^{2–5} Not surprisingly, surgical methods for achieving more quantitative cytoreduction are now receiving greater scrutiny.

Identification of malignant tissue during surgery is currently accomplished by three methods. First, many tumor masses and nodules can be visually detected based on abnormal color, texture, and/or morphology. Thus, a tumor mass may exhibit variegated color, appear asymmetric with an irregular border, or protrude from the contours of the healthy organ. A malignant mass may also be recognized tactiley due to differences in plasticity, elasticity, or solidity from adjacent healthy tissues. Finally, a few cancer foci can be located intraoperatively using fluorescent dyes that flow passively from the primary tumor into draining lymph nodes.^{6–9} In this latter methodology, fluorescent (sentinel) lymph nodes can be visually identified, resected, and examined to determine whether cancer cells have metastasized to these lymph nodes.

Even with the above tools for tumor identification, many malignant nodules still escape detection, leading to disease recurrence and often death.^{10–13} Motivated by a need for

improved tumor identification, two new approaches for intraoperative visualization of malignant disease have been introduced. In the first, a quenched fluorophore is injected systemically into the tumor-bearing animal, and release of the quenching moiety by a tumor-specific enzyme, pH change, or change in redox potential is exploited to selectively activate fluorescence within the malignant mass.^{14–20} In the second, a fluorescent dye is conjugated to a tumor-specific targeting ligand that causes the attached fluorophore to accumulate in cancers that overexpress the ligand's receptor. Examples of tumor targeting ligands used for this latter purpose include folic acid, which exhibits specificity for folate receptor (FR) positive cancers of the ovary, kidney, lung, endometrium, breast, and colon,^{21,22} and DUPA, which can deliver attached fluorophores selectively to cells expressing prostate-specific membrane antigen (PSMA), i.e., prostate cancers and the neovasculature of other solid tumors.^{23–25} Importantly, one folate-targeted fluorescent probe (folate-fluorescein or EC17) has been recently tested intraoperatively in human ovarian cancer patients.²⁶ In this study, ~5× more malignant lesions were removed with the aid of the tumor-targeted fluorophore than

Received: March 11, 2013

Revised: May 2, 2013

Published: May 5, 2013



without it, and all resected fluorescent lesions were confirmed by pathology to be malignant.

Unfortunately, a major deficiency with the above clinical study is derived from the fact that the attached dye (fluorescein) emits fluorescence in the visible range, i.e., where autofluorescence is strong and light penetrates tissue poorly.²⁷ Because light in the near-infrared (NIR) region induces little autofluorescence and permeates tissue much more efficiently, we wondered whether more complete tumor resection might be possible if an NIR dye were used to guide the surgery. To explore this possibility, we have synthesized several folate- and PSMA-targeted NIR probes and tested them for their abilities to image metastatic disease *in vivo*. In this article, we describe the synthesis, *in vitro* characterization, and relative abilities of various FR- and PSMA-targeted NIR probes to reveal metastatic disease in tumor-bearing mice.

EXPERIMENTAL PROCEDURES

Synthesis and Characterization of Folate- and DUPA-NIR Conjugates. All ligands and linkers were synthesized as previously reported.^{23,24,28–31} After purification, folate- and DUPA-targeting ligands were conjugated to selected NIR dyes as shown in Supporting Information, Schemes 1–3, to yield the final conjugates shown in Figure 1. NIR probes

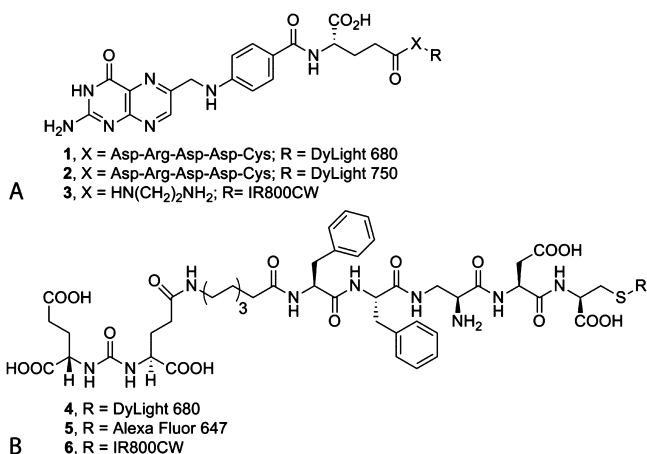


Figure 1. Tumor-targeted NIR probes. (A) Folate receptor-targeted NIR probes. (B) PSMA-targeted NIR probes.

were purified using reverse phase preparative HPLC [Waters, xTerra C18 10 μ m; 19 \times 250 mm; λ = 280 nm; solvent gradient, 0 to 30% or 80% B in a 30 min run; A = 10 mM NH₄OAc buffer in water (pH 7.0), and B = acetonitrile (ACN)]. Purified compounds were analyzed using LC-MS (ESI) mass spectrometry (Waters, X-Bridge C18 5 μ m; 3.0 \times 15 mm) (Supporting Information, Figures 1–6).

Culture of Folate and PSMA Receptor-Expressing Cells Lines. L1210A were obtained from Dr. Manohar Ratnam, and KB cells were obtained from American Type Culture Collection (ATCC; Rockville, MD). Cells were cultured in folate-deficient 1640 RPMI medium supplemented with 10% heat inactivated fetal bovine serum (HIFBS), 1% L-glutamine, and 1% penicillin-streptomycin (Invitrogen, Carlsbad, CA). All cell lines were cultured in 5% carbon dioxide and 95% air-humidified atmosphere at 37 °C.

LNCaP cells were obtained from ATCC and grown in RPMI-1640 medium containing 10% HIFBS, sodium pyruvate (100 mM), and 1% penicillin streptomycin. 22RV1 cells were

obtained from Dr. Michael Henry and cultured in RPMI-1640 containing 10% HIFBS, 1% MEM nonessential amino acids (GIBCO, Carlsbad, CA), and 1% Geneticin (Invitrogen, Carlsbad, CA).

Analysis of Binding Affinity and Specificity of Folate- and DUPA-NIR Probes. KB or LNCaP cells (200,000 cells/well in 500 μ L) were seeded into 24-well plates and allowed to form monolayers over 48 h. Spent medium in each well was replaced with fresh medium (0.5 mL) containing increasing concentrations of a folate- or DUPA-NIR probe in the presence or absence of 100-fold excess competing ligand, i.e., folic acid or 2-(phosphonomethyl)-pentanedioic acid (PMPA) (Axxora Platform, San Diego, CA), respectively. After incubating for 1 h at 37 °C, cells were rinsed with fresh medium (3 \times 0.5 mL), dissolved in 1% aqueous SDS (0.600 mL), and assayed for fluorescence by transfer to a quartz cuvette, and analysis of fluorescence emission intensity at each dye's excitation and emission maximum was performed using an Agilent Technologies Cary Eclipse fluorescence spectrophotometer. The conjugate's dissociation constant (K_d) was calculated by plotting fluorescence emission units versus the concentration of targeted NIR probe using GraphPad Prism 4.03.

In Vivo Mouse Models of Metastasis. All animal procedures were carried out with the approval of the Purdue Animal Care and Use Committee. For studies involving FR-expressing tumors, 5–6 week old female DBA/2 mice were purchased from Harlan Laboratories (Indianapolis, IN) and placed on a folate-deficient diet for two weeks prior to and during each study. For studies involving PSMA-expressing tumors, 5 week old male athymic nu/nu mice were purchased from Harlan Laboratories (Indianapolis, IN) and maintained on normal rodent chow for the duration of the study. Tumor metastases were induced by injecting 1×10^6 L1210A (FR expressing) or 22RV1 (PSMA expressing) cells into the left ventricle of the heart using a 30 gauge needle. Tumors were allowed to develop for 4 weeks, after which the animals were injected intravenously with 10 nmols of the desired FR- or PSMA-targeted NIR probe dissolved in 100 μ L of saline. After 4 h, animals were sacrificed by CO₂ asphyxiation and imaged as described below.

Fluorescent Imaging of Mice with Metastatic Disease. Animal imaging experiments were performed using a Caliper Ivis Lumina II Imaging Station with Living Image 4.0 software. Settings for imaging Alexa Fluor 647 and DyLight 680 conjugates were as follows: lamp level, high; excitation, 605; emission, Cy5.5; epi illumination; binning, (M) 4; FOV = 7.5; f-stop = 4; and acquisition time = 1 s. Settings for imaging DyLight 750 and IR800CW conjugates were as follows: lamp level, high; excitation, 745; emission, ICG; epi illumination; binning, (M) 4, FOV = 12.5; f-stop = 4; acquisition time = 1 s.

H&E Staining of Normal and Diseased Tissues. After imaging, organs were dissected and stored in 5 mL of formalin and submitted to Purdue Histology & Phenotyping Laboratory for H&E staining. In brief, tissue samples were processed using a Sakura Tissue-Tek VIP 6, sectioned using a Thermo Finesse ME microtome, and stained with H&E reagent using a Shandon Vari-Stain 24-2 autostainer. H&E stained slides were then imaged using an Olympus BH-2 research microscope with an Olympus DP70 camera.

RESULTS

Synthesis of Tumor-Targeted NIR Probes. For selective tumor targeting, we conjugated commercially available NIR dyes to either folate or DUPA (i.e., two tumor-targeting ligands shown previously to deliver attached therapeutic and imaging agents selectively to folate receptor- and PSMA-expressing tumors, respectively). Most folate- and DUPA-NIR probes (Figure 1) were synthesized at high yield and subsequently purified using HPLC to homogeneity.

Binding Affinity and Specificity of Targeted NIR Probes. Because the cargo attached to a ligand can often interfere with ligand binding, it was important to test the binding affinities of the folate- and DUPA-NIR probes to FR- and PSMA-expressing cells, respectively (Figure 2). Binding

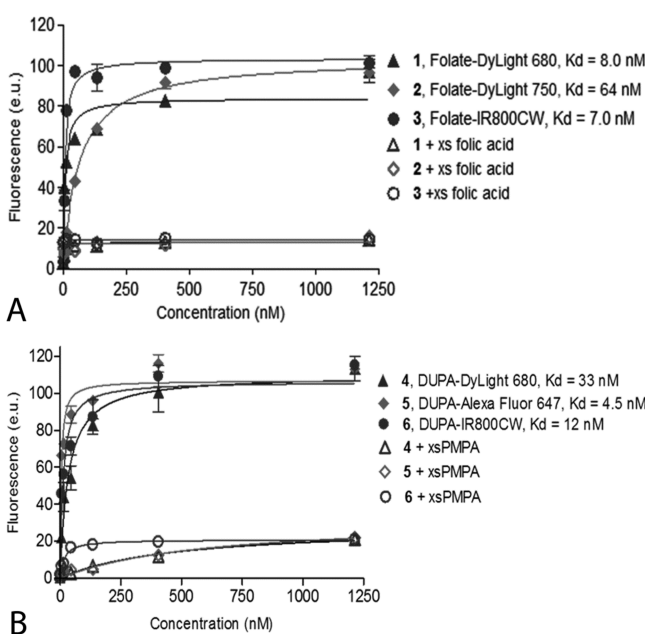


Figure 2. Binding isotherms of folate- and DUPA-NIR probes to cultured cancer cells. (A) Binding curves of folate-NIR probes to folate receptor-expressing KB cells in the presence (filled symbols) and absence (open symbols) of 100-fold molar excess folic acid. The targeted conjugates are DyLight 680 (triangles), Alexa Fluor 750 (diamonds), and IR800CW (circles). (B) Binding curves of DUPA-NIR probes to PSMA expressing LNCaP cells in the presence (filled symbols) and absence (open symbols) of 100-fold molar excess PMPA. The targeted conjugates are DyLight 680 (triangles), Alexa Fluor 647 (diamonds), and IR800CW (circles).

affinities of all conjugates were found to be in the low nanomolar range with some variation depending on the attached dye, suggesting that the linked cargo only mildly influences ligand binding. The specificity of folate- and DUPA-NIR probes for their receptors was also determined *in vitro* by adding excess folic acid and PMPA, respectively, to compete for all empty receptor binding sites. As seen in Figure 2, binding was nearly quantitatively inhibited by coincubation with 100-fold molar excess of competitor.

Imaging of Tumor-Targeted NIR Probes *in Vivo*. Because of the above differences in receptor binding affinities, as well as the observed heterogeneities in tumor size, microenvironment, and vascularity in our metastatic tumor models, we were not confident that we could obtain a quantitative comparison of the optical properties of our

tumor-targeted fluorophores in our live mouse models. Therefore, prior to evaluation of the tumor specificities of the tumor-targeted probes *in vivo*, we elected to compare the intensities of the selected dyes following excitation through porcine tissue *in vitro*. For this purpose, 1 mL of phosphate buffered saline containing 100 nM each of dye (Alexa Fluor 647, DyLight 680, DyLight 750, and IR800CW) was placed in an Eppendorf tube, which in turn was positioned under a 1 cm thick section of fresh porcine muscle, and the resulting tissues were imaged under the same conditions in both a Kodak Image Station and an IVIS Lumina Imager; only the optimal excitation and emission wavelengths were always selected for each dye in each instrument. As shown in Supporting Information, Figures 7 and 8, IR800CW produced the brightest fluorescent signal, with DyLight 750 yielding a signal of intermediate intensity and Alexa Fluor 647 and DyLight 680 displaying the weakest fluorescence.

In order to evaluate the abilities of the above folate- and DUPA-NIR probes to detect metastatic tumor nodules *in vivo*, a murine model of tumor metastasis was developed that involved intracardiac injection of 10^6 L1210A or 22RV1 cells (FR and PSMA expressing cells, respectively), followed by normal husbandry of the mice for 4 weeks to allow nascent tumors to grow. Tumor-bearing mice were then treated with 10 nmol of selected folate- or DUPA-NIR probe via tail vein injection, and mice were euthanized 4 h later for fluorescence imaging. As seen in Figure 3, tumor loci could be readily

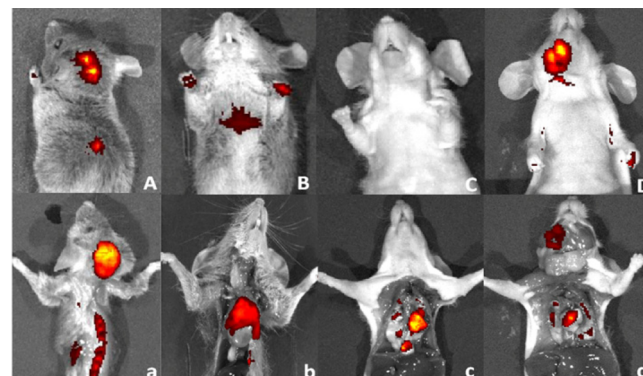


Figure 3. Fluorescent images of mice with metastatic disease 4 h following intravenous injection of folate- and DUPA-NIR probes. Fluorescent and white light image overlays of intact (A–D) and surgically opened (a–d) tumor-bearing mice. Mice (DBA/2 strain) with FR-expressing L1210A tumors were injected intravenously with 10 nmol of folate-DyLight 680 (A/a) or folate-DyLight 750 (B/b) and imaged 4 h later. Mice (athymic nu/nu strain) with PSMA-expressing 22RV1 tumors were injected intravenously with 10 nmol of either DUPA-DyLight 680 (C/c) or DUPA-Alexa Fluor 647 (D/d) and imaged 4 h later.

distinguished, yielding strong contrast between fluorescent cancer nodules and adjacent healthy tissues. In some cases, fluorescent tumors could even be seen in images of intact mice (Figure 3, top panels); however, due to differences in tumor size, location, and depth, it was not possible to unequivocally establish which NIR probe yielded the best images in intact animals.

Finally, in order to mimic a live surgical setting, resection of fluorescent tumor tissue was performed in stages, with the largest masses being removed first and smaller malignant loci being excised after more prominent fluorescent masses had

been cleared (Figures 4 and 5). Importantly, removal of the primary masses often revealed secondary metastases that were

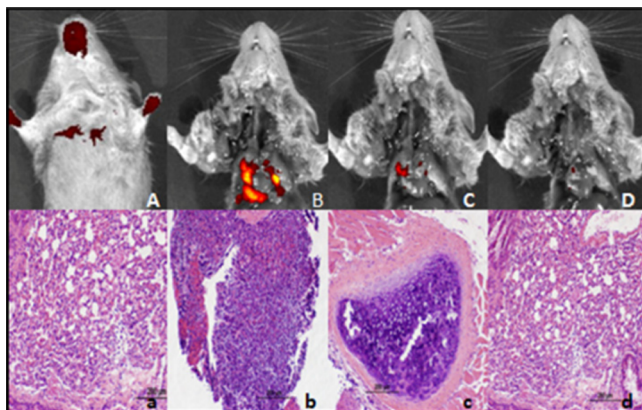


Figure 4. H&E analysis of tissue resected during sequential tumor debulking surgery. (A–D) Fluorescent and white light image overlays of L1210A tumor-bearing mice 4 h following tail vein injection with 10 nmol of folate-IR800CW. (A) Whole body image. (B) Opened chest cavity. (C) After the removal of primary tumor. (D) After the removal of all secondary nodules. (a–d) H&E staining of a, healthy control lung; b, primary tumor; c, secondary tumor nodule; and d, residual tissue.

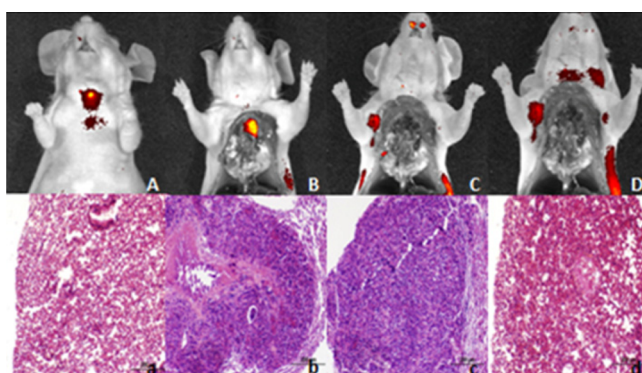


Figure 5. H&E analysis of tissue resected during sequential tumor debulking surgery. (A–D) Fluorescent and white light image overlays of 22RV1 tumor-bearing mice 4 h following tail vein injection with 10 nmol DUPA-IR800CW. (A) Whole body image. (B) Opened chest cavity. (C) After the removal of the primary tumor. (D) After the removal of all secondary nodules. (a–d) H&E staining of a, healthy control lung; b, primary tumor; c, secondary tumor nodule; and d, residual tissue.

not visible prior to the initial rounds of surgery and would have likely been missed without the aid of the tumor-specific fluorescence. Following these multiple rounds of resection, when all visible fluorescence had been removed, excised tissues were submitted for histological analysis, and these studies revealed that all fluorescent nodules were indeed malignant. More importantly, random sampling of the remaining tissues demonstrated that nonfluorescent regions were nonmalignant (Figures 4d and 5d), suggesting an apparent quantitative removal of cancerous lesions with the aid of the tumor-targeted fluorescent probes.

■ DISCUSSION

Two promising approaches to fluorescence-guided surgery are currently under intense investigation for use in the clinic. In

one method, an activatable NIR fluorescent probe, which is minimally fluorescent in the steady state due to its proximity to an attached quencher, becomes highly fluorescent upon release of the quencher in malignant tissue. One of the most commonly used release mechanisms involves incorporation of a peptide sequence between the dye and the quencher that can be specifically cleaved by a tumor-enriched protease (i.e., cathepsins, caspases and matrix metalloproteinases).^{32–36} A major advantage of this strategy lies in the absence of fluorescence in tissues that lack the activating enzyme, allowing tissues along the excretion pathway (e.g., kidneys, bladder, and liver) to remain nonfluorescent unless they fortuitously express the cleaving enzyme. Such tumor-activated NIR probes can also generate substantial fluorescence in the tumor mass as long as the malignant lesion is enriched in the cleaving protease and the released fluorophore is retained in the tumor.³⁷ The major disadvantage of this methodology arises from the poor tumor specificities of many of the relevant hydrolases (most of which are also expressed in healthy tissues undergoing natural remodeling or experiencing inflammation). Moreover, the abundance of the desired proteases may vary among tumor masses, leading to slow or no activation of fluorescence in some malignant lesions and rapid development of fluorescence in others.³⁸

The second method involves conjugation of an NIR dye to a tumor-specific targeting ligand that binds avidly to cancer cells and clears quantitatively from most healthy tissues. Advantages of this approach include (i) the rapid rate of tumor visualization, owing to the fact that tumor uptake and normal tissue clearance of the fluorophore can occur within minutes of intravenous injection, (ii) the stability of tumor contrast, arising from the fact that the ligand–dye conjugates are commonly internalized by the cancer cells via receptor-mediated endocytosis, (iii) the specificity of the fluorescence whenever the targeted receptor is either absent, weakly expressed, or inaccessible in normal tissues, and (iv) the absence of “bleeding” of fluorescence from malignant into nonmalignant tissues, due to high affinity retention of the ligand–dye conjugate on its receptor, creating highly defined boundaries that clearly demarcate the cancer. An obvious disadvantage of the strategy derives from the fact that the ligand-targeted NIR probe is always fluorescent, even during excretion, preventing imaging of kidney and bladder tumors until excretion of the fluorophore is complete.

One surprising result from our studies was the lower size of malignant lesions that could be readily detected *in vivo*. Thus, more detailed analyses of several sites with punctate metastatic disease revealed that cancer cell clusters as small as 50 μm could be visualized with the use of higher resolution optics. Because clusters of even a few cells can eventually lead to recurrence of the cancer, the ability to detect and remove even the smallest metastatic lesions could eventually lead to reduced patient mortality, assuming an appropriate camera can be designed.

While most applications of fluorescence-guided surgery likely remain to be discovered, some uses of the technology can already be envisioned. First, more malignant lesions will potentially be identified and resected due to better visualization of tumor masses. Second, in cases where maximal preservation of normal tissues is essential (i.e., cancers of the brain, breast, pancreas, head and neck, etc.), careful shaving of fluorescent lesions until no fluorescence remains might enable more efficient conservation of healthy tissue. Third, preoperative

staging of cancer patients might eventually be possible via laparoscopic interrogation of proximal lymph nodes for fluorescent lesions, obviating the need for surgery when significant metastases are clearly observed and eliminating the requirement for subsequent surgical sampling of sentinel lymph nodes when only a single tumor mass is detected.

In conclusion, we have demonstrated that tumor-targeted NIR probes have the potential to reshape standard surgical procedures by improving visualization of malignant tissues, leading to more complete and precise diseased tissue removal and improved patient outcome. Further studies will, however, be necessary to better define how this potentially powerful tool might best serve surgeons and patients alike.

■ ASSOCIATED CONTENT

Supporting Information

Detailed synthetic schemes and NIR dye tissue penetration studies. This material is available free of charge via the Internet at <http://pubs.acs.org>.

■ AUTHOR INFORMATION

Corresponding Author

*Tel: 765-494-5273. Fax: 765-494-5272. E-mail: plow@purdue.edu.

Present Addresses

[‡]Department of Chemistry, Indian Institute of Technology Indore, Indore-452017, Madhya Pradesh, India.

[§]On Target Laboratories, LLC, 1281 Win Hentschel Boulevard, West Lafayette, Indiana 47906, United States.

Notes

The authors declare no competing financial interest.

■ ACKNOWLEDGMENTS

This work was supported by research grants from Endocyte, Inc. and On Target Laboratories, LLC.

■ REFERENCES

- (1) De Grand, A. M., and Frangioni, J. V. (2003) An operational near-infrared fluorescence imaging system prototype for large animal surgery. *Technol. Cancer Res. Treat.* 2, 553–562.
- (2) Griffiths, C. T. (1975) Surgical resection of tumor bulk in the primary treatment of ovarian carcinoma. *J. Natl. Cancer Inst. Monogr.* 42, 101–104.
- (3) Bristow, R. E., Tomacruz, R. S., Armstrong, D. K., Trimble, E. L., and Montz, F. J. (2002) Survival effect of maximal cytoreductive surgery for advanced ovarian carcinoma during the platinum era: A meta-analysis. *J. Clin. Oncol.* 20, 1248–1259.
- (4) Karakiewicz, P. I., Eastham, J. A., Graefen, M., Cagiannos, I., Stricker, P. D., Klein, E., Cangiano, T., Schroder, F. H., Scardino, P. T., and Kattan, M. W. (2005) Prognostic impact of positive surgical margins in surgically treated prostate cancer: multi-institutional assessment of 5831 patients. *Urology* 66, 1245–1250.
- (5) Kapp, K. S., Kapp, D. S., Poschauko, J., Stucklschweiger, G. F., Hackl, A., Pickel, H., Petru, E., and Winter, R. (1999) The prognostic significance of peritoneal seeding and size of postsurgical residual in patients with stage III epithelial ovarian cancer treated with surgery, chemotherapy and radiotherapy. *Gynecol. Oncol.* 74, 400–407.
- (6) Kitai, T., Inomoto, T., Miwa, M., and Shikayama, T. (2005) Fluorescence navigation with indocyanine green for detecting sentinel lymph nodes in breast cancer. *Breast Cancer* 12, 211–215.
- (7) Tagaya, N., Yamazaki, R., Nakagawa, A., Abe, A., Hamada, K., Kubota, K., and Oyama, T. (2008) Intraoperative identification of sentinel lymph nodes by near-infrared fluorescence imaging in patients with breast cancer. *Am. J. Surg.* 195, 850–853.
- (8) Fujiwara, M., Mizukami, T., Suzuki, A., and Fukamizu, H. (2009) Sentinel lymph node detection in skin cancer patients using real-time fluorescence navigation with indocyanine green: preliminary experience. *J. Plast. Reconstr. Aesthet. Surg.* 62, E373–E378.
- (9) Ogasawara, Y., Ikeda, H., Takahashi, M., Kawasaki, K., and Doihara, H. (2008) Evaluation of breast lymphatic pathways with indocyanine green fluorescence imaging in patients with breast cancer. *World J. Surg.* 32, 1924–1929.
- (10) Bristow, R. E. (2000) Surgical standards in the management of ovarian cancer. *Curr. Opin. Oncol.* 12, 474–480.
- (11) Rubin, S. C., Randall, T. C., Armstrong, K. A., Chi, D. S., and Hoskins, W. J. (1999) Ten-year follow-up of ovarian cancer patients after second-look laparotomy with negative findings. *Obstet. Gynecol.* 93, 21–24.
- (12) Yossepovitch, O., Bjartell, A., Eastham, J. A., Graefen, M., Guillonneau, B. D., Karakiewicz, P. I., Montironi, R., and Montorsi, F. (2009) Positive surgical margins in radical prostatectomy: Outlining the problem and its long-term consequences. *Eur. Urol.* 55, 87–99.
- (13) Khouri-Collado, F., and Chi, D. S. (2011) Recent surgical management of ovarian cancer. *J. Obstet. Gynaecol. Res.* 37, 379–382.
- (14) Weissleder, R., Tung, C. H., Mahmood, U., and Bogdanov, A., Jr. (1999) *In vivo* imaging of tumors with protease-activated near-infrared fluorescent probes. *Nat. Biotechnol.* 17, 375–387.
- (15) Urano, Y., Asanuma, D., and Hama, Y. (2009) Selective molecular imaging of viable cancer cells with pH-activatable fluorescence probes. *Nat. Med.* 15, 104–109.
- (16) Mahmood, U., and Weissleder, R. (2003) Near-infrared optical imaging of proteases in cancer. *Mol. Cancer Ther.* 2, 489–496.
- (17) Hama, Y., Urano, Y., Koyama, Y., Gunn, J. R., Choyke, P. L., and Kobayashi, H. (2007) A self-quenched galactosamine-serum albumin-rhodamineX conjugate a ‘smart’ fluorescent molecular imaging probe synthesized with clinically applicable material for detecting peritoneal ovarian cancer metastases. *Clin. Cancer Res.* 13, 6335–6343.
- (18) Ogawa, M., Kosaka, N., Choyke, P. L., and Kobayashi, H. (2009) *In vivo* molecular imaging of cancer with a quenching near-infrared fluorescent probe using conjugates of monoclonal antibodies and indocyanine green. *Cancer Res.* 69, 1268–1272.
- (19) Bremer, C., Bredow, S., Mahmood, U., Weissleder, R., and Tung, C. H. (2001) Optical imaging of matrix metalloproteinase-2 activity in tumors: feasibility study in a mouse model. *Radiology* 221, 523–529.
- (20) Mahmood, U., Tung, C. H., Bogdanov, A., Jr., and Weissleder, R. (1999) Near-infrared optical imaging of protease activity for tumor detection. *Radiology* 213, 866–870.
- (21) Parker, N., Turk, M. J., Westrick, E., Lewis, J. D., Low, P. S., and Leamon, C. P. (2005) Folate receptor expression in carcinomas and normal tissues determine by a quantitative radioligand binding assay. *Anal. Biochem.* 338, 284–293.
- (22) Xia, W., and Low, P. S. (2010) Folate-targeted therapies for cancer. *J. Med. Chem.* 53, 6811–6824.
- (23) Kularatne, S. A., Wang, K., Santhapuram, H. K. R., and Low, P. S. (2009) Prostate-specific membrane antigen targeted imaging and therapy of prostate cancer using a PSMA inhibitor as a homing ligand. *Mol. Pharmaceutics* 6, 780–789.
- (24) Kularatne, S. A., Zhou, Z., Yang, J., Post, C. B., and Low, P. S. (2009) Design, synthesis and preclinical evaluation of prostate-specific membrane antigen targeted ^{99m}Tc-radioimaging agents. *Mol. Pharmaceutics* 6, 790–800.
- (25) Chang, S. S., Reuter, V. E., Heston, W. D., Bander, N. H., Grauer, L. S., and Gaudin, P. B. (1999) Five different anti-prostate-specific membrane antigen (PSMA) antibodies confirm PSMA expression in tumor-associated neovasculature. *Cancer Res.* 59, 3192–3198.
- (26) van Dam, G. M., Themelis, G., Crane, L. M., Harlaar, N. J., Pleijhuis, R. G., Kelder, W., Sarantopoulos, A., de Jong, J. S., Arts, H. J., van der Zee, A. G., Bart, J., Low, P. S., and Ntziachristo, V. (2011) Intraoperative tumor-specific fluorescence imaging in ovarian cancer by folate receptor-α targeting: first in-human results. *Nat. Med.* 17, 1315–1320.

- (27) Kennedy, M. D., Jallad, K. N., Thompson, D. H., Ben-Amotz, D., and Low, P. S. (2003) Optical imaging of metastatic tumors using a folate-targeted fluorescent probe. *J. Biomed. Opt.* 8, 636–641.
- (28) Leamon, C. P., Reddy, J. A., Vlahov, I. R., Westrick, W., Parker, N., Nicoson, J. S., and Vetzel, M. (2007) Comparative preclinical activity of the folate-targeted vinca alkaloids conjugates EC140 and EC14S. *Int. J. Cancer.* 121, 1585–1592.
- (29) Leamon, C. P., Reddy, J. A., Vlahov, I. R., Kleindl, P. J., Vetzel, M., and Westrick, E. (2006) Synthesis and biological evaluation of EC140: a novel folate-targeted vinca alkaloid conjugate. *Bioconjugate Chem.* 17, 1226–1232.
- (30) Vlahov, I. R., Santhapuram, H. K., Kleindl, P. J., Howard, S. J., Stanford, K. M., and Leamon, C. P. (2006) Design and regioselective synthesis of a new generation of targeted therapeutics. Part 1, EC14S, a folic acid conjugate of desacetylvinblastine monohydrate. *Bioorg. Med. Chem. Lett.* 16, 5093–5096.
- (31) Lu, Y., and Low, P. S. (2002) Folate targeting of haptens to cancer cell surfaces mediated immunotherapy of syngeneic murine tumors. *Cancer Immunol. Immunother.* 51, 153–162.
- (32) Zhu, L., Zhang, F., Ma, Y., Liu, G., Kim, K., Fang, X., Lee, S., and Chen, X. (2011) *In vivo* optical imaging of membrane-type matrix metalloproteinase (MT-MMP) activity. *Mol. Pharmaceutics* 8, 2331–2338.
- (33) Tung, C. H., Bredow, S., Mahmood, U., and Weissleder, R. (1999) Preparation of a cathepsin D sensitive near-infrared fluorescence probe for imaging. *Bioconjugate Chem.* 10, 892–896.
- (34) Bremer, C., Tung, C. H., and Weissleder, R. (2001) *In vivo* molecular target assessment of matrix metalloproteinase inhibition. *Nat. Med.* 7, 743.
- (35) Tung, C. H., Mahmood, U., Bredow, S., and Weissleder, R. (2000) *In vivo* imaging of proteolytic enzyme activity using a novel molecular reporter. *Cancer Res.* 60, 4953–4958.
- (36) Tung, C. H. (2004) Fluorescent peptide probes for *in vivo* diagnostic imaging. *Biopolymers* 76, 391–403.
- (37) Nguyen, Q. T., Olson, E. S., Aguilera, T. A., Jiang, T., Scadeng, M., Ellies, L. G., and Tsien, R. Y. (2010) Surgery with molecular fluorescence imaging using activatable cell-penetrating peptides decreases residual cancer and improves survival. *Proc. Natl. Acad. Sci. U.S.A.* 107, 4317–4322.
- (38) Bremer, C., Tung, C. H., Bogdanov, A., and Weissleder, R. (2002) Imaging of differential protease expression in breast cancers for detection of aggressive tumor phenotypes. *Radiology* 222, 814–818.